Available online at www.sciencedirect.com

ScienceDirect

Advances in Space Research 69 (2022) 254–265

ADVANCES IN SPACE RESEARCH (a COSPAR publication)

www.elsevier.com/locate/asr

Effect of 21 June 2020 solar eclipse on the ionosphere using VLF and GPS observations and modeling

Gaurish Tripathi [a], S.B. Singh [a], Sanjay Kumar [a], Ashutosh K. Singh [b], Rajesh Singh [c], A.K. Singh [a,*]

[a] Atmospheric Research Lab., Department of Physics, Banaras Hindu University, Varanasi 221005, India
[b] Faculty of Physical Sciences, Shri Ramswaroop Memorial University, Lucknow-Dewa Road, Barabanki, India
[c] KSK Geomagnetic Research Laboratory, IIG, Prayagraj, UP, India

Received 17 July 2021; received in revised form 14 October 2021; accepted 8 November 2021
Available online 12 November 2021

Abstract

A solar eclipse event provides a great opportunity to examine the behavioral concept of the ionospheric electron density (N_e) variability in the low latitude region. The current work presents our outcomes from the simultaneous assessment of Tweeks (radio atmospherics) and radio signals (fixed frequency of the transmitter's signal) from multifarious VLF transmitters observed at Varanasi (Geog. Lat. 25.27^{0}N, Geog. Long. 82.98^0 E, Geomag. Lat. 14^0 55′N). To find the presence of disturbances in the ionosphere Global Positioning System (GPS) data at Hyderabad (geog. lat. 17^0 20$^/$ N, long. 78^0 30$^/$ E) and Bangalore (geog. lat. 12^0 58$^/$ N, long. 77^0 33$^/$ E) is also analyzed during the period of the solar eclipse on 21 June 2020. As the Sun was eclipsed, the nighttime phenomenon of 'Tweeks' was also observed in the daytime through the annular solar eclipse due to nighttime conditions as the solar disc was dusked. Tweek analysis shows the variation in the ionospheric reflection heights (∼8–11 km) and electron density (∼3–2 cm^{-3}) in the D-region during the eclipse. The reflection height of the D-region ionosphere increases from ∼84 km and goes to ∼95 km and then decreases to ∼87 km. Electron concentration (electron density) decreased throughout the eclipse from 24 cm^{-3} to 21 cm^{-3} and then increases to 23 cm^{-3}. Eclipse-imposed modifications in VLF transmitter's (HWU and NWC) signals displays an average change (decrease) of 2.8 dB and 0.8 dB in the signal strength of 18.3 kHz (HWU) and 19.8 kHz (NWC) transmitters respectively and a rise in virtual reference height (H′) and sharpness factor (β), as compared with normal days. The de-trended value of total electron content (DTEC) variations at both stations clearly shows the presence of travelling ionospheric disturbances (TIDs) having wave-like features. The Fast Fourier Transform (FFT) analysis shows that periodicity at both the station lies in two regimes one belongs to a period between 20 and 50 min and the other belongs to 50–90 min indicating such oscillation observed in the ionosphere are induced by atmospheric gravity waves (AGWs) generated during the period of the solar eclipse.

Keywords: Solar eclipse; D-region ionosphere; Electron density; VLF waves; Tweeks

1. Introduction

Events like solar eclipse show a significantly short time effect on the local ionospheric properties, that's why it is of great interest for the ionospheric radio science community. During a Solar Eclipse (SE), the ionospheric electron density concentration is sharply reduced to a level near night-time values. This affects radio communication

* Corresponding author at: Atmospheric & Space Physics Research Lab, Department of Physics, Banaras Hindu University, Varanasi 221 005, India.
E-mail address: singhak@bhu.ac.in (A.K. Singh).

https://doi.org/10.1016/j.asr.2021.11.007
0273-1177/

through the ionosphere and produces a disturbance in satellite navigation (Smith, 1972; Singh et al., 2011).

Extensive researches have been done on solar eclipse to study its effects on ionospheric parameters (Klobuchar and Whitney, 1965; Singh et al., 2011; Kumar and Singh, 2012), meteorological parameters (Anderson et al., 1972), total columnar ozone (Chakrabarty et al., 1997; Zerefos et al., 2000), boundary layer physics (Antonia et al., 1979), photochemistry (Srivastava et al., 1982; Zanis et al., 2007) and gravity wave (Chimonas and Hines, 1970; Zerefos et al., 2007). 'Eclipses' are different based on occurrence time of the year, the solar disk occultation degree, time of the day, atmospheric weather, and location (latitude and longitude) of observations on the earth (Baran et al., 2003). But still, due to the rare happening of solar eclipses, reported works are limited. Hence, each solar eclipse, depending upon its time of occurrence, duration, and geographical location has a particular impact on the earth's ionosphere. Through the solar eclipse (SE), there is a blockage of solar ionizing radiation which creates a night-time situation and results in a decrease of electron density over the shadow region (Clilverd et al., 2001). The changes in the electron density distribution have been studied using different techniques such as the ionosonde networks (Venkatesh et al., 2011), incoherent scatter radars (Zhang et al., 2004), GPS systems (Kumar et al., 2013), VLF transmitters (Singh et al., 2012) and satellite measurements (Davies and Hartman, 1997). A network of GPS receivers and VLF receivers distributed over the whole globe provides a better opportunity to study the ionospheric variations. Ionospheric measurement during solar eclipse gives an important consideration for the investigation of ionospheric perturbation. Mitra (1948) has observed the perturbation of the ionosphere through the eclipse and reported the smooth decrease in ionization as the eclipse progressed.

The impact on the lower ionosphere especially on D-region due to eclipse can be considered with the Very Low Frequency (VLF) radio wave signal modulation observations. The naturally occurred VLF radio signals and fixed frequency (narrowband signals) from various VLF transmitters across the world are considered very important tools for continuous monitoring of the D-region ionosphere. These VLF signals travel through the Earth-ionosphere waveguide (EIWG) by the multiple reflections, which are formed by the Earth and the lower ionosphere (Clilverd et al., 2001, Kumar et al., 2008; Singh et al., 2011). During a solar eclipse, the change in VLF propagation through the earth-ionosphere waveguide is highly dependent on path length, location of the totality spot concerning the path, frequencies, and other parameters (Cohen et al., 2018).

Tweeks (radio atmospherics) are formed mainly during night hours, as lightning-generated ELF-VLF waves propagate to long-distance in the Earth-ionosphere waveguide (EIWG) with low attenuation (Yamashita, 1978; Singh and Singh, 1996). The first tweek's observations during a total solar have been reported by Burton and Boardman (1933) at Conway, New Hampshire on 31 August 1932. Rycroft and Reeve (1970) have investigated about 60 tweeks during a total solar eclipse (TSE) in Newfoundland Canada on 7 March 1970 and determined the variation in the ionospheric reflection heights through the eclipse. They concluded that there was a rise of reflection heights about 7 km above the normal daytime. Singh et al. (2011) has observed tweeks with higher harmonics ($n > 1$) at low latitude stations Allahabad and Nainital in the Indian sector through the total solar eclipse on 22 July 2009. From the first cut-off frequency of the tweeks, the variations in VLF reflection height of about 5 km and electron density (22–23 cm^{-3}) have been reported in the D-region ionosphere through the total solar eclipse on 22 July 2009. Studies on the solar eclipse also report a remarkable change in phase and amplitude perturbations in ELF/VLF radio signals propagating inside the EIWG related during solar eclipses (Lynn, 1981; Buckmaster and Hansen, 1998; Clilverd et al., 2001). Zhang et al. (2011) have examined the VLF signals detected at Nanjing, China, and found anomalous changes in the intensity of the VLF signal through the total solar eclipse on 22nd July 2009, showing the consequence alike to the sunrise and sunset. Some studies are on 22 July 2009 TSE effects collectively using broadband (300 Hz to 30 kHz) and narrowband (fixed frequency) VLF signal observations (e.g., Guha et al., 2010; Kumar et al., 2016; Ohya et al., 2012; Phanikumar et al., 2014; Singh et al., 2011; Zhang et al., 2011).

Solar eclipse not only affects the D-region of the ionosphere but also affects the E and F-regions (Kumar et al., 2013). The state of the ionosphere is very much dependent on the radiation coming from the Sun and loss of sunlight due to solar eclipse make nighttime condition and hence affect the production of ionization in the ionosphere. In the last decade's ionospheric TEC using ground-based GPS based measurements are being used to study the variations of the ionosphere during the solar eclipse (Le et al., 2008; Kumar and Singh, 2012; Kumar et al., 2013; Kumar et al., 2016; Silwal et al., 2021). Using ground-based GPS-TEC data at Varanasi, Kanpur, Hyderabad, and Bangalore Kumar et al. (2013) have shown 30–54% reduction in TEC at Indian stations during the total solar eclipse of 22 July 2009. Using electron density profile from satellite-based COSMIC RO measurements; they have further shown a reduction in electron density from 100 to 800 km altitude with a maximum of ~48% at 360 km altitude (F-region). Recently Rao et al. (2021) have studied the TEC reduction during the tail phase of the 21st June 2020 annular solar eclipse and reported a decrease in TEC values at all chosen stations in the Chinese-Taiwanese region after the eclipse onset which reach the lowest value a few minutes afterward the eclipse maximum phase.

Thus, to study the effect of the solar eclipse on the low latitude ionosphere simultaneously by using both VLF measurements and GPS measurements at multi-station is lacking. To complete this gap the present study has been initiated based on analysis of VLF measurements at Varanasi (Geog. Lat. 25.27^{0}N, Geog. Long. 82.98^0 E, Geomag. Lat. 14^0 55$^/$ N) and GPS measurements at Hyderabad (geog. lat. 17^0 20$^/$ N, long. 78^0 30$^/$ E) and Bangalore (geog. lat. 12^0 58$^/$ N, long. 77^0 33$^/$ E). The VLF signals transmitted from NWC, Australia (at 19.8 kHz) and HWU, France (at 18.3 kHz) are recorded in Varanasi and are used to find any significant variations in the amplitude and phase of the VLF signal. The tweeks are also used to find the variation in ionospheric parameters such as electron density, the height of reflection from normal behaviour during eclipse. The GPS measured of DTEC is used to find oscillation observed in the ionosphere induced by atmospheric gravity waves (AGWs) generated during the period of the solar eclipse. The experimental setups and data analysis are presented in Section 2. Section 3 presents the description of the eclipse and the main observations. Section 4 discusses observed results and their discussions. Finally, Section 5 concludes the study.

2. Experimental setup and analysis

2.1. VLF measurements

The continuous broadband and narrowband digital VLF recording are done by the Automatic Whistler Detector and Analyzer (AWDA) system installed at the Department of Physics, Banaras Hindu University Varanasi since December 2010. AWDA system worked on the algorithm which has been used to remove the unwanted signals and power line harmonics (Lichtenberger et al., 2008). The antenna of the AWDA is crossed magnetic loop (Lichtenberger et al., 2008; Singh et al., 2014) and with the area, ~100 m^2 orientated geomagnetic north–south and east–west so that the receiver picks up magnetic fields parallel to the ground from any directions. The installed antenna is also sensitive to receive the navigational transmitter's VLF signals. There is the synchronization of the PC time with the Pulse Per Second (PPS) signal of a GPS receiver. The accuracy of the timing of PPS is better than 1 μs, it is less than the data sampling period (~22 μs) (Lichtenberger et al., 2008).

A user-level program *sampler.i386* has been used in the installed instrument AWDA, which communicates with Jacked upon start-up and also writes data on the disk and opens a file every hour. False detection can occur if specific local noises appear or a close storm generates a 'sferics curtain' spoiling all signals (Lichtenberger et al., 2008). A detailed description of the AWDA is found in the previous papers (Lichtenberger et al., 2008; Singh et al, 2014; Singh et al, 2019).

The naturally occurred VLF waves are mainly produced by lightning strokes (Arnold and Pierce, 1964) and detected by sensitive receivers at any location on the Earth due to preoperational loss inside the Earth-ionosphere waveguide about a few dB/Mm (Nagano et al., 2007). The received waves give a useful description of the generation of the lightning-producing mechanism and as well as the characteristics of the propagation medium.

Through the solar eclipse campaign period 21–23 June 2020, the VLF data at Varanasi was recorded in continuous mode. These sampled data are examined by codes developed in MATLAB. There are two types of data recording: broadband data and narrowband data. The broadband data contains a continuous spectrum (300 Hz–47.5 kHz) of VLF waves which contain various types of emissions like sferics, tweeks, etc. While the recordings of narrowband data have a variation of phase and amplitude of the fixed frequency VLF transmitter signals.

2.2. GPS-TEC measurements

GPS observations data downloaded from the International Global Navigation Satellite System (GNSS) Services (IGS) website (https://cddis.nasa.gov/archive/gnss/data) provide slant total electron content (STEC) along the line of observation point from the concerned satellite. The STEC data with a time resolution of 30 s is converted into vertical total electron content (VTEC) according to the relation discussed elsewhere (Kumar & Singh, 2009). It is important to note that the error in VTEC computation from STEC could be very large for lower elevation angles due to the multipath effect and tropospheric scattering due to water vapor, etc. Therefore, to reduce this error in VTEC, only those satellite signals are considered which have a high enough elevation angle (>70°). The high elevation cut-off allows only those GPS signals with ionospheric pierce points at 350 km altitude and above near the ground GPS receiver (Kumar et al., 2015).

2.3. Observations

The annular phase of 21 June 2020 was a rare solstice solar eclipse, seen from parts of Africa and Asia, including the Central African Republic, Congo, Ethiopia, southern Pakistan, northern India, and China. This rare solstice "ring of fire" eclipse had a long path, but it was also very narrow and figured out across 14 countries and two continents, Africa and Asia. Even in West Africa, the broadening of the path was only about 85 km. Here, annularity was remained for about 1 min and 20 s.

In India (in Uttarakhand) near the border of China and Nepal, at the location of the greatest eclipse, the magnitude of the eclipse was 0.996 and the path was about 21 km wide. Annularity was remained here for around 38 s. Among all the annular solar eclipses between 2003 and 2031, this eclipse had the highest magnitude (0.994) at the instant of the Greatest Eclipse. The occurrence activity of this solar eclipse at Varanasi is shown in Table 1. Considering the Earth as a whole, the partial phase of the eclipse started at 9:15:58 hrs IST (Indian Standard Time; IST = UT + 5.50 hrs). The annularity begins at 10:17:45

Table 1
Local circumstances for the Varanasi on June 21, 2020.

Events	Time (IST) in Varanasi.	Altitude (deg)	Azimuth (deg)
Partial eclipse begins	21 Jun, 09:15:58	**69.6**	**090.7**
Maximum Eclipse	21 Jun, 12:10:04	**85.6**	**245.1**
Partial eclipse end	21 Jun, 15:04:01	**61.8**	**272.7**

(IST) and ended at 14:02:17 (IST). The partial phase ended at 15:04:01 (IST) and it has lasted about 3 h, 33 min, and 19 s. The solar eclipse visibility on 21 June 2020 at Varanasi was recorded to be 77.32 % (coverage of the Sun) and the Magnitude is 0.822. The annular solar eclipse path which was found on 21 June 2020 is mainly localized in the low latitude region and has been shown in Fig. 1. The VLF signal from NWC Australia (21.81^0 S; 114.16^0 E) is transmitted at 19.8 kHz and from HWU France (46.71^{0}N; 01.24^0 E) is transmitted at 18.3 kHz and both are received at the Varanasi India (25.31^{0}N; 82.97^0 E) and their great circle path is also shown in Fig. 1.

The great circle path of NWC to Varanasi passes over the southern low-latitude to the northern low-latitude, while the great circle path of HWU to Varanasi passes over mid-latitude to the low latitude region. Here the path lengths of VLF propagation from the receiving station for NWC and HWU are 10150 km and 6230 km respectively.

The typical VLF radio atmospherics/tweeks which were recorded by AWDA during the solar eclipse on 21 June 2020 is shown in Fig. 2. It shows four typical examples of tweeks (radio atmospherics) observed on the day of the solar eclipse at 06:45:41.9482 UT (12:15:41.9482 IST), 7:17:4.0476 UT (12:47:4.0476 IST), 15:19:0.8712 UT (20:49:0.8712 IST) and 17:36:57.9228 UT (23:06:57.9228 IST). Fig. 2(a) & 2(b) shows that the tweeks recorded during a solar eclipse (day time) have less dispersion and less intensity than the nighttime tweeks, as shown in Fig. 2(c) & 2(d).

In this paper, we have also examined variations of ionospheric TEC on solar eclipse days from ground-based GPS measurements**.** For this TEC data from two selected PRNs (PRN 02 and 06) are analyzed. The path of the solar eclipse along with the trajectory of Ionospheric Pierce Point (IPP) of PRNs 02 and 06 observed from Indian stations Hyderabad and Bangalore are shown in Fig. 3. The blue point with * marker inside blue circle on the path of the solar eclipse shows a great eclipse point (GEP). The GEP is defined as a position on path of the solar eclipse where duration of eclipse is greatest. Moreover GEP is the location where the annular eclipse lasts the longest along the entire path. The stations Hyderabad and Bangalore are marked by symbol * with red and blue color respectively. The Colour bar put on the right of the figure indicates the passage time of the eclipse and respective PRN in UT (Hour). The number put on the line plot indicates the

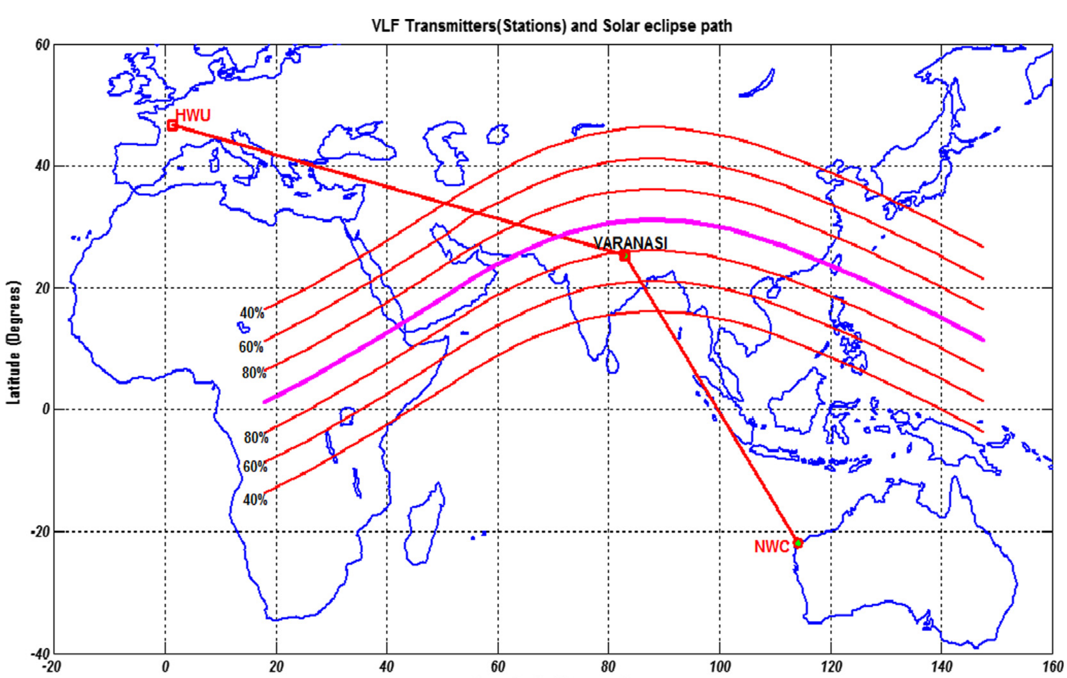

Fig. 1. Worldwide solar eclipse path on June 21, 2020, with percentage obscuration. Small circles show the location of VLF Transmitters (HWU, NWC) and receiving site, Varanasi.

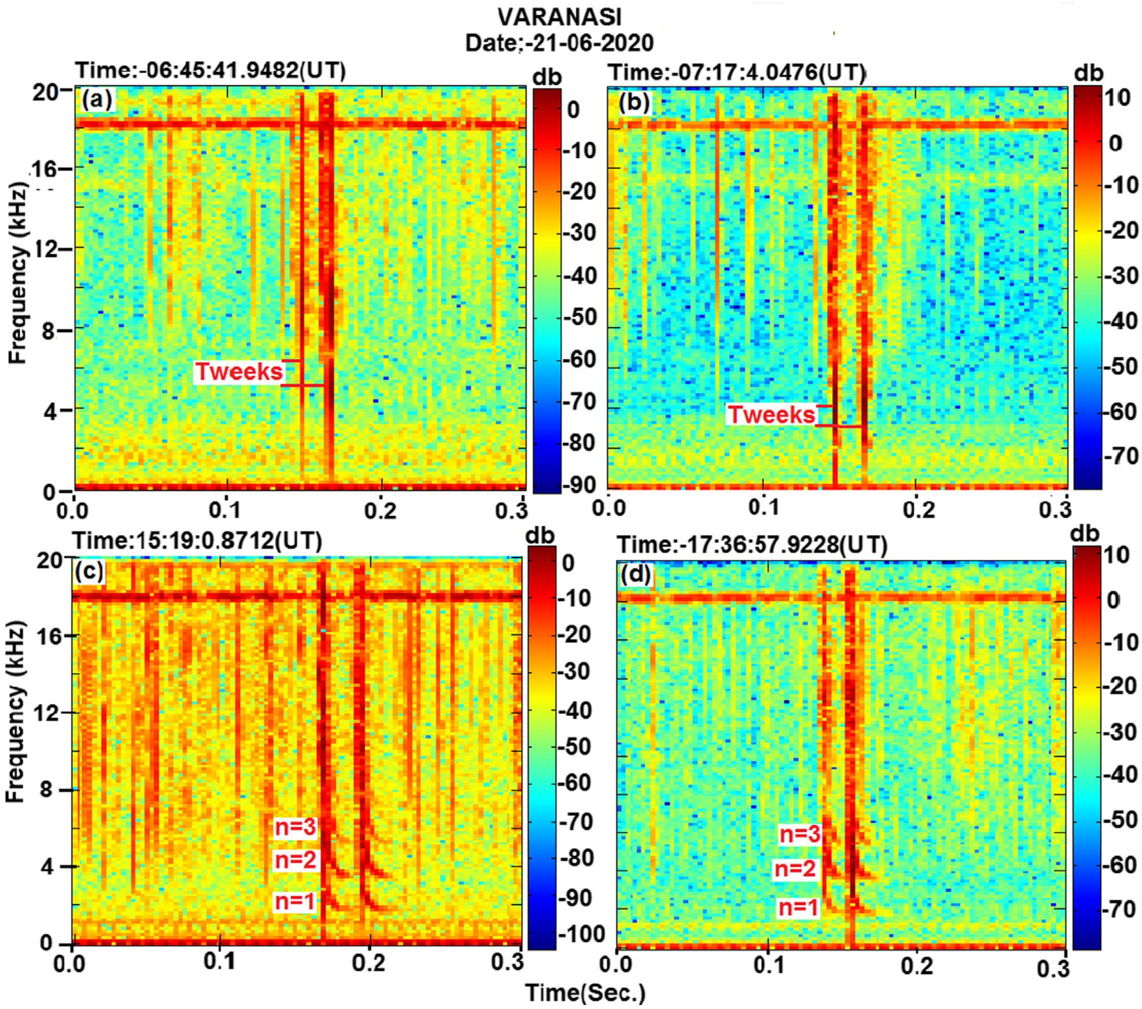

Fig. 2. The tweeks observed at Varanasi on 21 June 2020: (a & b) eclipse time tweeks, and (c &d) night time tweeks.

respective PRN. The results in detail from these PRNs are described in Fig. 9 (Section 4.2).

We have also examined geomagnetic activity on the eclipse day and found it low during this interval. On 21 June 2020 Dst-index was between −8nT and 2nT. One day before the eclipse and the day after the eclipse, the Dst-index was varied between −8 nT to 19 nT and −4nT to 8 nT respectively. The observation shows clearly that there is no definite evidence of changes in the currents flowing in the dynamo layer of the ionosphere.

3. Results and discussion

3.1. Results of VLF study

For observing the effect of the solar eclipse on the D-region ionosphere, we have analyzed the recorded tweeks and we modelled VLF transmitter signals to see parametric variations in the ionosphere throughout a solar eclipse (partial night condition). The long-distance propagation of the VLF is controlled by the status of the lower ionosphere and the conductivity of the Earth's surface (Cummer et al., 1998). The conductive ionosphere and the conductive Earth form a horizontal "duct", which acts as a waveguide confining the waves so the waves don't escape into space and the waves travel in a zig-zag path around the Earth, reflected alternately by the Earth and the ionosphere. The VLF waves propagate by TE and TM modes and the most widely considered mode for the estimation of EIWG properties is the TM mode inside the cavity of the ionosphere. The cut-off frequency (f_c) of each tweek is measured with precision and the ionosphere reflection height (h) is calculated using the equation $h = c/(2 f_c)$ (Yamashita, 1978), where 'c' is the velocity of light in free space. The electron density (n_e) at the reflection height (h) is determined by using the equation n_e (cm^{-3}) = 1.365 × 10^{-2} f_c (Ohya et al., 2003). For the low-latitude we have assumed electron gyrofrequency, $f_H = 1.1$ MHz (Ohya et al., 2003).

The first-order mode cut-off frequencies of the recorded tweeks are 1.5–1.7 kHz. The cut-off frequencies of the first harmonics of the tweeks are recorded from 9.30 IST (21-06-2020) to 5.30 IST (22-06-2020) and have been used to find the reflection height (h) and the electron density (n_e).

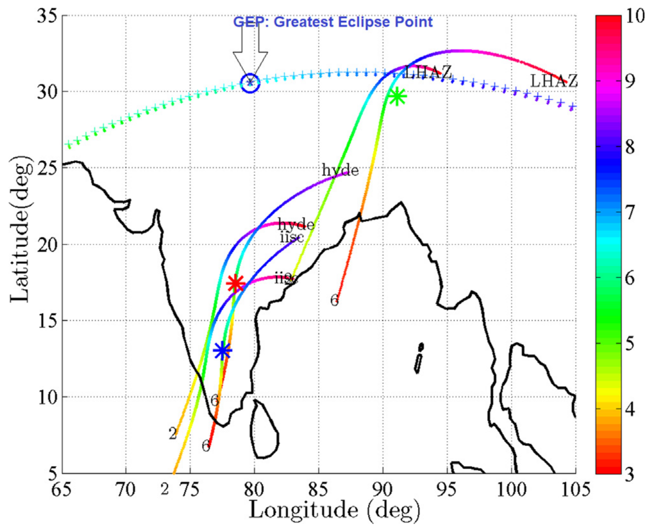

Fig. 3. Path of the solar eclipse of 21 June 2020 along with IPP of respective PRN 02 and 06 observed from Hyderabad (marked by *with red color) and Bangalore station (marked by * with blue color) on the day of the solar eclipse of 21 June 2020. The Colour bar put on the right of the figure indicates the passage time of respective PRN in UT (Hour). Numbers put on the line plot indicate the respective PRN. (For interpretation of the references to color in this figure legend, the reader is referred to the web version of this article.)

There flection height (h) of the ionosphere was found to be variable between 84 and 95 km and electron density (n_e) varied between 21 and 24 cm^{-3} and these variables are shown in Fig. 4. The calculated reflection height (h) and electron density (n_e) are shown by the upper and lower panel respectively. From Fig. 4, it is clear that reflection height (h) and electron density (n_e) vary from 9.30 am to 2.30 pm through the eclipse period, and this variation is because of the effect of the solar eclipse on the D-region of the ionosphere which reduces the ionization in the ionosphere. Hence observations show that when the solar eclipse started on 21 June 2020, a partial nighttime condition is created which results in observation of tweeks events.

Tweeks were observed at Varanasi just after the start of the eclipse because a transitory night-time propagation condition is created due to the recombination of electrons in the lower ionosphere which lowers the electron density to a post-sunset value.

Many authors have reported the effect of the solar eclipse on the ionosphere (Nymphas et al., 2009; West et al., 2008; Jakowski et al., 2008; Chen et al., 2010). It is expected that the strength of the signal will change during the eclipse event because VLF signals are reflected specifically at the D-layer of the Ionosphere. So, the fixed frequency of the VLF radio transmitted signals from the NWC (19.8 kHz) in North West Cape Australia and HWU (18.3 kHz) in Rosnay France have been also analysed and modelled to observe the solar eclipse effect on the D-region of the ionosphere. Many authors have studied the fixed frequency VLF transmitter's signal variation and several ionospheric parameters (Clilverd et al., 2001; Chernogor, 2010; Kaufmann and Schaal, 1968; Mendes Da Costa et al., 1995; De et al., 2008; De and Sarkar, 1997). They remarked that the amplitude strength of the VLF wave variation is due to the transient changes in the lower ionosphere caused by the solar eclipse.

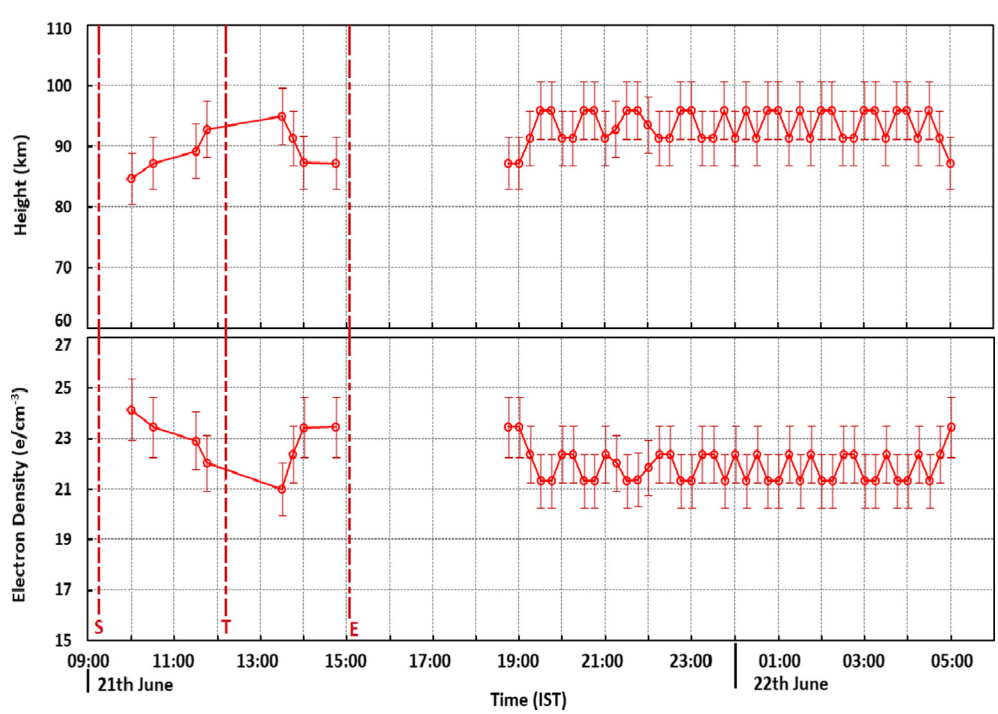

Fig. 4. The variation of reflection height (upper panel) and electron density (lower panel) with time observed at Varanasi on 21 June 2020, over 15 min intervals. The vertical line marked with M represents the maximum eclipse time and the line marked with E represents the end of the eclipse.

VLF transmitters signalsfrom HWU (18.3 kHz) and NWC (19.8 kHz) have been utilized to analyze the impacts of the solar eclipse on the propagation characteristics of VLF waves as well as anionospheric condition through the eclipse. Fig. 5 displays the diurnal variations of the VLF signal amplitude recorded at our station Varanasi from the HWU transmitter during 21–23 June 2020, while Fig. 6 displays diurnal variations of the VLF signal of the NWC-VNS path. The remarkable change in the amplitude of the signal is found during eclipse time approximately 10:45am to 02:00 pm. In finding the changes of the amplitude of VLF signals at a fixed location on Earth, the important role is played by the distance between the VLF transmitter and receiver, the geomagnetic conditions, and the conductivity of the lower ionosphere (Clilverd et al., 2001). Since the different propagation paths suffered different levels of obscuration so the duration of obscuration for each transmitter–receiver path may be different. The maximum changes in the VLF signal amplitude for HWU-Varanasi path is about 2.8 dB, while for NWC-Varanasi path it is about 0.8 dB at the time of the maximum obscuration of the eclipse and then attaining normal value at the end of the eclipse.

The variation in the amplitude of VLF transmitter signal during the eclipse has also been utilized to find the change in the apparent magnitude of the reflection coefficient. Bracewell (1952) has concluded the first time that the VLF signal is affected by the eclipse. As being governed by the temporary shadowing of the ionosphere under the effect of the eclipse, the effective reflection height of the ionosphere is affected by the electron density. Venkatesham et al. (2019) and Singh et al. (2012) have also utilized the VLF signal to analyze the effect on the D-region ionosphere through the total solar eclipse (TSE) on 22 July 2009. The amplitude of the VLF signal can increase or decrease during the eclipse due to the propagation path's interference. Many researchers (Singh et al., 2012; Maurya et al, 2014) have reported that the amplitude increases during TSE for the transmitter–receiver great circle path (TRGCP) parallel to the totality path. Clilverd et al. (2001) have reported for 11 August 1999 TSE about an increase and decrease in the amplitude of the VLF signal. A careful study of the events reported by different authors (Clilverd et al., 2001, Singh et al., 2012, Maurya et al., 2014) shows that only TRGCPs aligned parallel to the totality path and confined in the low equatorial region have an increase in the amplitude. As the TRGCPs of HWU-VNS and NWC-VNS were nearly perpendicular to the totality path and HWU being mid-latitude region, a decrease in the amplitude of the VLF signal is observed.

Cummer et al. (1998) has described an experimental profile equation to find the electron density at a height of h km, of the D-region ionosphere which is as follows:

$$Ne(h) = 1.43 \times 10^{7}\exp(-0.15H')\exp[(\beta - 0.15)(h - H')]cm^{-3} \quad (1)$$

where $H^{/}$ is the virtual reference height in km and β is the Wait inverse scale parameter in km^{-1} (Wait & Spies 1964, Thomson, 1993). The altitude profile and the sharpness of the ionosphere are controlled by the two main parameters $H^{/}$ and β. We have used the $H^{/} = 71$ km and $\beta = 0.43$ km^{-1}, for the unperturbed ionosphere (Thomson, 1993) for modelling. Derived values of these ionospheric parameters through the eclipse are found $H^{/} = 74.1$ km and $\beta = 0.458$ km^{-1} respectively. The graphs which are showing the variation of electron density is plotted in Fig. 7 with the help of obtained Wait's parameters during the eclipse for

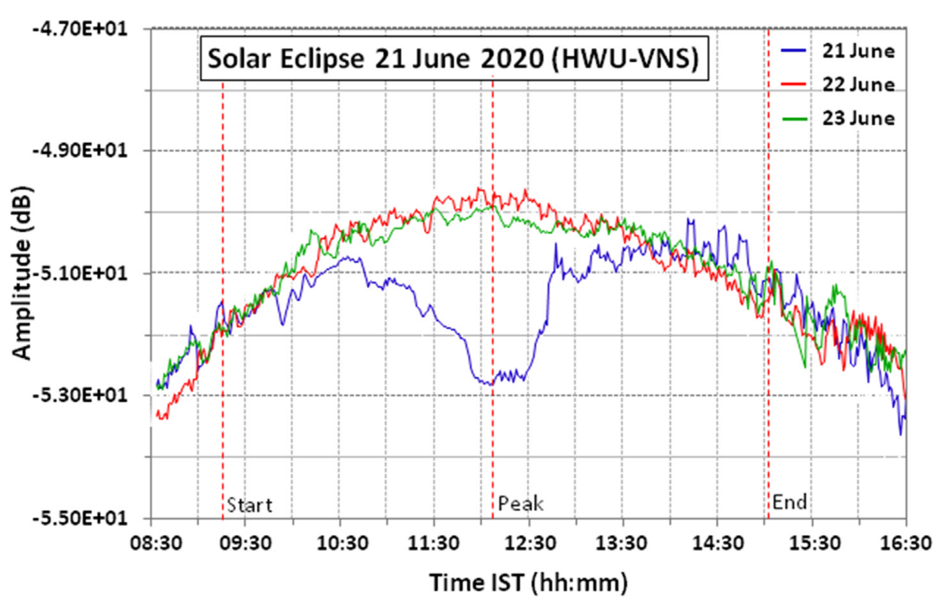

Fig. 5. The amplitude variation of HWU (18.3 kHz) VLF-signal at Varanasi during normal days and on 21 June 2020 annular SE day (blue line). (For interpretation of the references to color in this figure legend, the reader is referred to the web version of this article.)

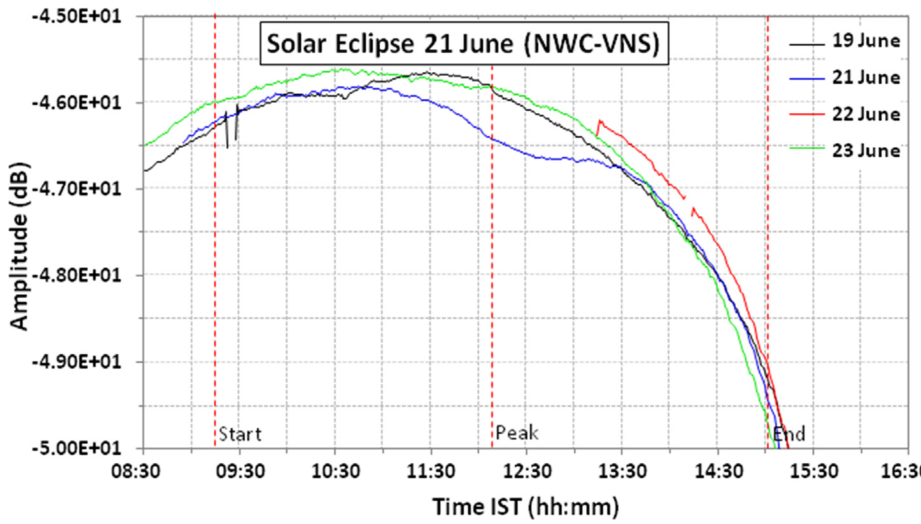

Fig. 6. The amplitude variation of NWC (19.8 kHz) VLF-signal at Varanasi during normal days and on 21 June 2020 annular SE day (blue line). (For interpretation of the references to color in this figure legend, the reader is referred to the web version of this article.)

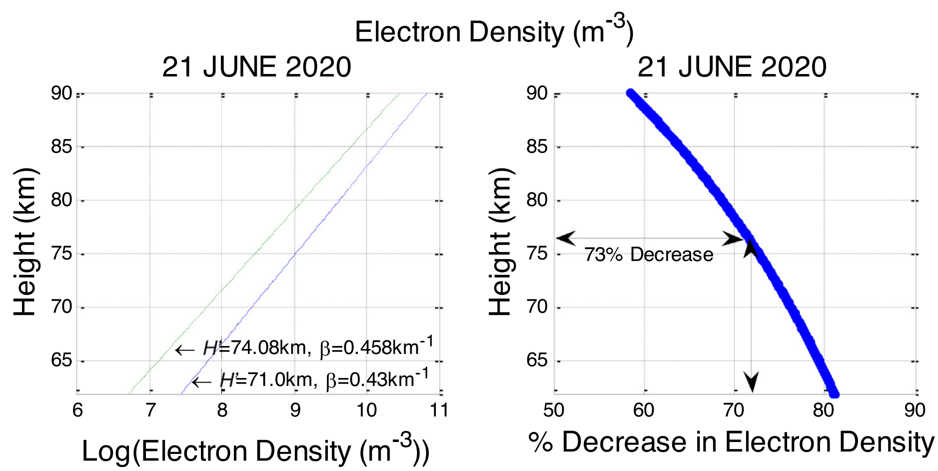

Fig. 7. Vertical profile of electron density (logarithmic scale) and variation of the percentage decrease in electron density with height for HWU-VNS path.

the unperturbed ionosphere. Clilverd et al. (2001) has reported that an average change of 1 dB in amplitude relatives to a change of $H^{/} = 1.1$ km and $\beta = 0.01$ km^{-1} (for short path less than 600 km). The variation in virtual reference height ($H^{/}$) and inverse scale parameter (β) have been also studied by Venkatesham et al. (2019) and Singh et al. (2012) using the transmitter signals on the solar eclipse 22 July 2009. They have concluded that $H^{/}$ and β are increased by 2.3 km, 0.02 km^{-1}, and 3.3 km, 0.03 km^{-1} respectively. In the present study, a decrease of 2.8 dB in signal strength is observed during the maximum solar obscuration over the HWU-Varanasi path, which results in an increase of about 3.1 km in virtual reference height, $H^{/}$ and 0.028 km^{-1} in β. Similarly, for the NWC transmitter, the VLF amplitude strength is found to decrease by 0.8 dB and the corresponding conductivity parameters $H^{/}$ and β are found to increase by 0.88 km and 0.008 km^{-1} respectively. Hence our observed decrease of signal strength and change in $H^{/}$ and β values agreed well with previously reported results (Guha et al., 2010; Venkatesham et al., 2019).

We have plotted the derived electron density profile from the computed value of $H^{/} = 74.1$ km and $\beta = 0.458$ km^{-1} with the unperturbed D-region ionosphere in Fig. 7 (Left panel). The corresponding % decrease in electron density relative to the height for the HWU – Varanasi path has also been plotted in Fig. 7 (Right panel). It shows that the average electron density at a reference height 77 km which is about 74 % less than the normal condition. The electron density decreases linearly with a rate of 0.69 %/km from the height of 65 to 80 km.

The derived electron density profile from the partially eclipsed values of $H^{/} = 71.8$ km and $\beta = 0.438$ km^{-1} along with the unperturbed D-region ionosphere have been plotted in Fig. 8 (Left panel) for the NWC-Varanasi path. The corresponding % change in the electron density concerning the height variation is plotted in Fig. 8 (Right panel). It displays that the average electron density at 77 km is around

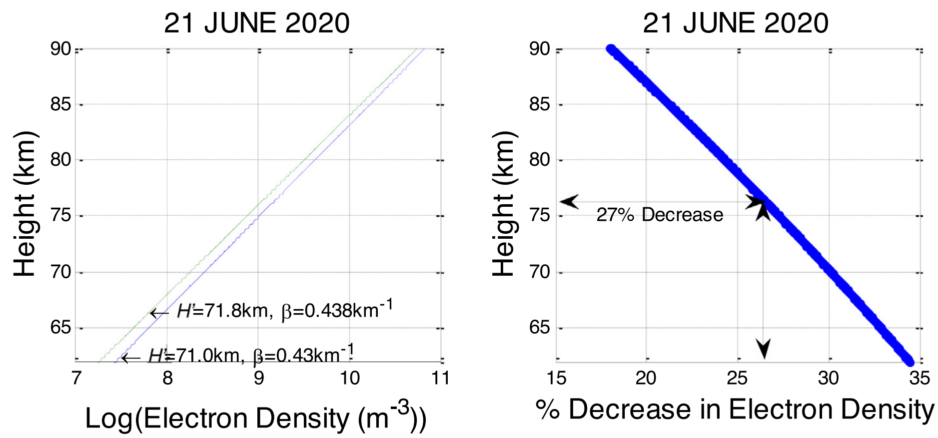

Fig. 8. Vertical profile of electron density (logarithmic scale) and variation of the percentage decrease in electron density with height for NWC-VNS path.

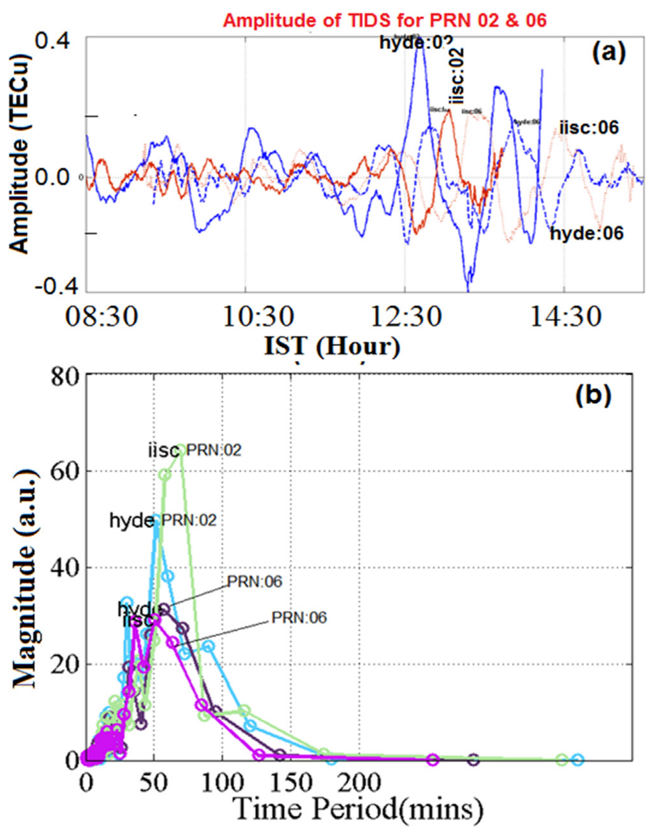

Fig. 9. (a) The amplitude of DTEC data of different PRN at Hyderabad and Bangalore station on solar eclipse day of 21 June 2020. The DTEC is obtained by taking the difference of VTEC of given PRN and its best-fit polynomial value. (b) FFT analysis of DTEC at Hyderabad and Bangalore showing periodicity.

27 % less compared to the normal condition. Here also electron density decreases linearly with a rate of 0.69 %/km from the height of 65 to 80 km. The results are steadied with the assumption of linear variation in electron production rate with solar ionizing radiation (Clilverd et al., 2001). The results show that the variation in the electron density and the amplitude of the VLF signal depends on the region of totality and path of traveling of VLF waves.

Singh et al. (2012) reported that because of reduced attenuation created by nighttime conditions, the received amplitude of the VLF signal is increased for stations located in the totality path and with TRGCP aligned parallel to the totality path. Contrary to our previous result on TSE (Singh et al., 2012), in the present analysis, the VLF amplitude is found to be decreased when TRGCP intersects perpendicularly to the totality path. This is because of modal interference at the receivers created by the discontinuity in the EIWG by the TSE. The mode theory (Budden, 1961; Wait and Spies, 1964) has explained that a fixed frequency VLF signal is a superposition of the electric field related with different modes from the transmitter and reaching the receiver point after being reflected and attenuated within the EIWG. The reflection of waves by the effective layer of the ionosphere varies with the electron densities of the layer. The solar flux is regulating the variation of electron distribution in the ionosphere and is represented by Wait's parameter (Wait and Spies, 1964).

3.2. Results of GPS study

In order to find the presence of disturbances in the ionosphere De-trended value of total electron content (DTEC) of VTEC data, GPS data at Hyderabad (HYDE) and Bangalore (IISC) for chosen PRN 02 and 06 are analyzed during the period of the solar eclipse on 21 June 2020. The PRN stands for a pseudo-random number which is the identity of each GPS satellite. The DTEC is obtained by taking the difference of VTEC and its best-fit polynomial value. The amplitude of DTEC and FFT of DTEC data are shown respectively from top to bottom in Fig. 9 (a, b). Fig. 9(a) shows the amplitude of DTEC variation for PRN 02 and 06 at Hyderabad and Bangalore during the solar eclipse of 21 June 2020. DTEC variations at both stations clearly show the presence of traveling ionospheric disturbances (TIDs) started at around 0855 IST having wave like features. To study wave features in more detail the periodicity of wave in VTEC can be obtained using the Fast Fourier Transform (FFT) analysis for PRNs 02 and

06 is carried out which is shown in Fig. 9(b). It is clear that periodicity at both the station lies in two regimes one belongs to a period between 20 and 50 min and the other belongs to 50–90 min indicating such oscillation observed in the ionosphere are induced by atmospheric gravity waves (AGWs) generated during the period of the solar eclipse. Solar eclipse affects the atmosphere and ionosphere through several processes and the partial/total termination of the solar flux affects chemical reactions, production/loss, and transport of ionization in the ionosphere (Sharma et al., 2010; Galav et al., 2010; Kumar and Singh, 2012), boundary layer phenomena (Jayakrishnan et al., 2013), and many other related phenomena including the generation and propagation of atmospheric gravity waves (Farges et al., 2003). During the solar eclipse, the moon's shadow travels with the supersonic speed in the atmosphere which generates atmospheric gravity waves (AGW's) in the lower atmosphere that would propagate upward and can be observed as traveling ionospheric disturbances (TID's) in the ionosphere region (Chimonas and Hines, 1970). The waves are excited in the lower atmosphere which gains large amplitudes and can reach the thermosphere and ionosphere (Hines, 1960). Depending upon the source, the periodicities of AGWs varying between 30 min and 3 h with a horizontal velocity between 400 and 1000 m/s have been reported in previous works (Prölss, 1993; Hocke and Schlegel 1996; Bauske and Prölss, 1997; Ding et al., 2007). Using GPS-TEC data for other cases of solar eclipse reported period of GWs are 20 mins to more than 100 mins (Kumar et al., 2013; Manju et al., 2014; Vijay Kumar et al. 2016; Nayak and Yigit 2018). For the total solar eclipse of 22 July 2009 of duration about 2 h, using GPS-TEC data at EIA station Allahabad Vijay Kumar et al. (2016) reported a period of gravity wave between 20 and 45 mins and 70–90 mins and further argued that shorter period corresponds to morning terminator and longer period corresponds to solar eclipse induced AGWs. They have further shown that period of AGWs increases when moving from D-region to F-region of the ionosphere. Using chain of GPS stations, for total solar eclipse of 21 August 2017 period of GWs in ionosphere 20–90 mins has been reported (Nayak and Yigit 2018). Using foF2 observations from ionosonde, Manju et al. (2014) reported wave periods of 30–100 mins during an annular eclipse of 15 January 2010 of 90% obscuration. Present analysis also reports period of GWs 20–90 mins at level of ionosphere which falls within above reported results. Moreover the period of GWs observed in the ionosphere may vary with measurements techniques used as different techniques have different temporal resolution. In present analysis GPS-TEC data with high temporal resolution of 30 s have been used.

4. Conclusion

During the annular solar eclipse of 21 June 2020, the recorded VLF measurements at low latitude stations Varanasi and GPS measurements at Hyderabad and Bangalore- are used in the present work to study the ionospheric perturbations. The new results of both the observations and LWPC modelling have been presented and discussed.

VLF radio atmospherics/tweeks sere recorded at Varanasi during the solar eclipse of June 21, 2020. The occurrence of tweeks which are nighttime phenomena was observed during the solar eclipse period and stopped at the end of the eclipse. The ionospheric reflection height increases from 84 km to 95 km at the totality and then decreases at the end of the eclipse. The reflection height of the D-region of the ionosphere rises to about 11 km indicating that there is a reduction in D-region ionization during the eclipse.

During the annular solar eclipse of 21 June 2020, the LWPC modeling of the D region ionosphere displayed a modest (0.8–3.1 km) rise in average virtual reference height. The reduction in electron density for the NWC-VNS path is found 27 %, which is lower as compared to the 74% decrease for the HWU-VNS path. The ionospheric virtual reference height $H^{/}$ has different values for different TRGCPs. The $H^{/}$ is increased by 3.1 km for HWU-Varanasi GCP passing over the central line of totality and is increased by 0.8 km for NWC-Varanasi GCP. The evaluated values of the β and $H^{/}$ derived for mid-latitude transmitting signal station HWU (18.3 kHz) and Varanasi path are found to be 0.458 km^{-1} and 74.1 km respectively. Similarly, the evaluated values of the β and $H^{/}$ for low latitude station transmitting signal station NWC (19.8 kHz) and Varanasi path are found to be 0.438 km^{-1} and 71.8 km respectively. The variation in the amplitude strength of the VLF signals of HWU (18.3 kHz) and NWC (19.8 kHz) during the eclipse is found to be 2.8 dB and 0.8 dB respectively compared with the corresponding normal day's values. Our observed outcomes of the decrease in the signal strength and an increase in $H^{/}$ and β agree well with the previous worker's results. It is mainly notable that our outcomes of reflection height variation through the eclipse, obtained by two different methods (tweeks analysis and VLF modeling) display a good acceptance of the outcomes from similar measurements.

The analysis of TEC data of selected PRNs from ground-based GPS measurements at two Indian stations Hyderabad and Bangalore shows the presence of traveling ionospheric disturbances (TIDs) having wave-like signatures. The periodicity of TIDs lies in two regimes one of which belongs to a period between 20 and 50 min and the other belongs to 50–90 min. Such oscillations observed in the ionosphere are induced by atmospheric gravity waves (AGWs) generated during the period of the solar eclipse. Decrease in the ionospheric electron density and hence change in the reflection height of the D-region ionosphere during eclipse is demonstrated by VLF modelling and tweek analysis. The TIDs generated in the upper atmosphere regime during eclipse also confirms sudden change in ionospheric electron density.

Declaration of Competing Interest

The authors declare that they have no known competing financial interests or personal relationships that could have appeared to influence the work reported in this paper.

Acknowledgment

The work is partially supported by SERB, New Delhi for the CRG project (File No: CRG/2019/000573) and partially by the Institute of Eminences (IoE) (Scheme no: 6031) grant to BHU. The author SBS is thankful to the DST-PURSE (5050) grant for providing a Research Associate. GPS observations data are downloaded from the IGS website (https://cddis.nasa.gov/archive/gnss/data). SK is thankful to CSIR New Delhi for assisting Scientist Pool Scheme [13(9049-A)/2019- Pool]. We are thankful the both the reviewers for their valuable comments and suggestions.

References

Anderson, R.C., Keefer, D.R., Myers, O.E., 1972. Atmospheric pressure and temperature changes during the 7 March 1970 solar eclipse. J. Atmos. Sci. 29, 583–587.

Antonia, R.A., Chambers, A.J., Phong-Anant, D., Rajagopalan, S., Sreenivasan, K.R., 1979. Response of atmospheric surface layer turbulence to a partial solar eclipse. J. Geophys. Res. 4, 1689–1692.

Arnold, H.R., Pierce, E.T., 1964. Leader and junction processes in the lightning discharge as a source of VLF atmospherics. Radio Sci. 68D, 771–776.

Baran, L.W., Ephishov, I.I., Shagimuratov, I.I., Ivanov, V.P., Lagovsky, A.F., 2003. The response of the ionospheric total electron content to the solar eclipse on 11 August 1999. Adv. Space Res. 31 (4), 989–994.

Bauske, R., Prölss, G.W., 1997. Modeling the ionospheric response to traveling atmospheric disturbances. J. Geophys. Res. 102, 14555–14562.

Bracewell, R.N., 1952. Theory of formation of an ionospheric layer below E layer based on eclipse and solar flare effects at 16 kc/sec. J. Atmos. Terr. Phys. 2, 226–235.

Buckmaster, H.A., Hansen, C.H., 1998. 26 February 1996 total solar eclipse induced LF (60kHz) phase retardation. J. Atmos. Terr. Phys. 48, 393–397.

Budden, K.G., 1961. The Wave-guide Mode Theory of Wave Propagation. Logos Press, London.

Burton, E., Boardman, E., 1933. Effects of Solar Eclipse on Audio Frequency Atmospherics. Nature 131, 81–82.

Chakrabarty, D.K., Shah, N.C., Pandya, K.V., 1997. Fluctuation in ozone column over Ahmadabad during the solar eclipse of 24 October 1995. Geophys. Res. Lett. 24 (23), 3001–3003.

Chernogor, L.F., 2010. Variations in the amplitude and phase of VLF radio waves in the ionosphere during the August 1, 2008, solar eclipse. Geomagn. Aeron. 50 (1), 96–106.

Chimonas, G., Hines, C.O., 1970. Atmospheric Gravity waves induced by a solar eclipse. J. Geophys. Res. 75, 5545–5551.

Chen, G., Zhou, Z., Yang, G., Zhang, Y., 2010. Solar eclipse effects of 22 July 2009 on sporadic E. Ann. Geophysicae 28, 353–357.

Clilverd, M.A., Rodger, C.J., Thomson, N.R., Lichtenberger, J., Steinbach, P., Cannon, P., Angling, M.A., 2001. Total solar eclipse effects on VLF signals: Observations and modeling. Radio Sci. 36 (4), 773–788.

Cohen, M.B., Gross, N.C., Higginson-Rollins, M.A., Marshall, R.A., Gołkowski, M., Liles, W., et al., 2018. The lower ionospheric VLF/LF response to the 2017 Great American Solar Eclipse observed across the continent. Geophys. Res. Lett. 45, 3348–3355.

Cummer, S.A., Inan, U.S., Bell, T.F., 1998. Ionospheric D region remote sensing using VLF radio atmospherics. Radio Sci. 33, 1781–1792.

Davies, K., Hartman, G.K., 1997. Studying the ionosphere with global positioning system. Radio Sci. 32, 1695–1703.

De, B.K., Sarkar, S.K., 1997. Anomalous behaviour of 22.3 kHz NWC signal during total solar eclipse. Kodaikanal Obs. Bull 13, 205–208.

De, S.S., De, B.K., Bandyopadhyay, B., Sarkar, B.K., Paul, S., Haldar, D. K., Barui, S., Datta, A., Paul, N., 2008. The effects of solar eclipse of August 1, 2008 on Earth's atmospheric parameters. Pure Appl. Geophys. 167, 1273–1279.

Ding, F., Wan, W., Ning, B., Wang, M., 2007. Large-scale traveling ionospheric disturbances observed by GPS total electron content during the magnetic storm of 29–30 October 2003. J. Geophys. Res. 112, A06309.

Farges, T., Pichon, A. Le, Blanc, E., Perez, S., Alcoverro, B., 2003. Response of the lower atmosphere and the ionosphere to the eclipse of August 11, 1999. J. Atmos. Solar-Terr. Phys. 65, 717–726.

Galav, P., Sharma, S., Pandey, R., January 2010. Total electron content in peninsular India during the eclipse of 15 January 2010. Curr. Sci. 99, 731–732.

Guha, A., De, B.K., Roy, R., Choudhury, A., July 2009. Response of the equatorial lower ionosphere to the total solar eclipse of 22 July 2009 during sunrise transition period studied using VLF signal. J. Geophys. Res. 115, A11302.

Hines, C.O., 1960. Internal atmospheric gravity waves at ionospheric heights. Can. J. Phys. 38 (11), 1441–1481.

Hocke, K., Schlegel, K., 1996. A review of atmospheric gravity waves and travelling ionospheric disturbances: 1982–1995. Ann. Geophys. 14 (9), 917–940.

Jakowski, N., Stanko, S.M., Wilken, V., Borries, C., Altadill, D., Chum, J., Buresova, D., Boska, J., Sauli, P., Hurska, F., Cander, L.R., 2008. Ionospheric behavior over Europe during the solar eclipse of 3 October 2005. J. Atmos. Sol. Terr. Phys. 70 (6), 836–853.

Jayakrishnan, P.R., Babu, C.A., Sivaprasad, P., 2013. Drastic variation in the surface boundary layer parameters over Cochin, during the Annular Solar Eclipse: Analysis using sonic anemometer data. J. Atmos. Solar-Terr. Phys. 94, 49–53.

Kaufmann, P., Schaal, R.E., 1968. The effect of a total solar eclipse on long path VLF transmission. J. Atmos. Terr. Phys. 30, 469–471.

Klobuchar, J.A., Whitney, H.E., 1965. Ionospheric electron content measurement during solar eclipse. J. Geophys. Res. 70, 1254.

Kumar, S., Kumar, A., Ramachandran, V., 2008. Higher harmonic tweek sferics observed at low latitude: estimation of VLF reflection heights and tweek propagation distance. Ann. Geophysicae 26, 1451–1459.

Kumar, S., Singh, A.K., 2009. Variation of ionospheric total electron content in Indian low latitude region of equatorial ionization anomaly (EIA). Adv. Space. Res 43, 1555–1562.

Kumar, S., Singh, A.K., 2012. Changes in total electron content (TEC) during the annular solar eclipse of 15 January 2010. Adv. Space Res. 49, 75–82.

Kumar, S., Tan, Eng Leong, Murti, D.S., 2015. Impacts of solar activity on performance of the IRI-2012 model predictions from low to mid latitudes. Earth Planet Space 67, 42.

Kumar, S., Inan, U., Maurya, A.K., Singh, R., 2016. Changes in the D region associated with three recent solar eclipses in the South Pacific region. J. Geophys. Res. Space Phys. 121, 5930–5943.

Kumar, S., Singh, A.K., Singh, R.P., 2013. Ionospheric Response to Total Solar Eclipse of 22 July 2009 at different Indian Regions. Ann. Geophys. 31, 1549–1558.

Le, H.J., Liu, L.B., Yue, X.A., Wan, W.X., 2008. The midlatitude F2 layer during solar eclipses: Observations and modeling. J. Geophys. Res.: Space Phys. 113 (A8), A08309.

Lynn, K.J.W., 1981. The total solar eclipse of 23 October 1976 observed at VLF. J. Atmos. Terr. Phys. 43, 1309–1316.

Lichtenberger, J., Ferencz, C., Bodnár, L., Hamar, D., Steinbach, P., 2008. Automatic Whistler Detector and Analyzer system: Automatic Whistler Detector. J. Geophys. Res. 113, A12201.

Manju, G., Madhav Haridas, M.K., Ramkumar, G., Pant, T.K., Sridharan, R., Sreelatha, P., 2014. Gravity wave signatures in the dip equatorial ionosphere-thermosphere system during the annular solar eclipse of 15 January 2010. J. Geophys. Res. Space Phys. 119, 4929–4937. https://doi.org/10.1002/2014JA019865.

Maurya, A.K., Phanikumar, D.V., Singh, R., Kumar, S., Vennadhari, B., Kwak, Y.S., Kumar, A., Singh, A.K., Kumar, K., 2014. N, Low-mid latitude D region ionospheric perturbations associated with 22 July 2009 total solar eclipse: Wave-like signatures inferred from VLF observations. J. Geophys. Res. Space Physics 119 (10), 8512–8523.

Mendes Da Costa, A., Leme, N.M.P., Piazza, L.R., June 1992. Lower ionosphere effect observed during the 30 June 1992 total solar eclipse. J. Atmos. Terr. Phys. 57, 13–17.

Mitra, S.K., 1948. Geomagnetic control of region F2 of the ionosphere. Nature 158, 668–669.

Nagano, I., Yagitani, S., Ozaki, M., Nakamura, Y., Miyamura, K., 2007. Estimation of lightning location from single station observations of sfer-ics. Electron. Commun. Jpn., Part I 90 (1), 25–34.

Nayak, C., Yigit, August 2017. GPS-TEC observation of gravity waves generated in the ionosphere during 21 August 2017 total solar eclipse. J. Geophys. Res. Space Phys. 123, 725–738. https://doi.org/10.1002/2017JA024845.

Nymphas, E.F., Adeniyi, M.O., Ayoolai, M.A., Oladiran, E.O., 2009. Micrometeorological measurements in Nigeria during the total solar eclipse of 29 March, 2006. J. Atmos. Sol. Terr. Phys. 71 (12), 1245–1253.

Ohya, H., Nishino, M., Murayama, Y., Igarashi, K., 2003. Equivalent electron density at reflection heights of tweek atmospherics in the low-middle latitude D-region ionosphere. Earth Planets Space 55, 627–635.

Ohya, H., Tsuchiya, F., Nakata, H., Shiokawa, K., Miyoshi, Y., Yamashita, K., Takahashi, Y., 2012. Reflection height of daytime tweek atmospherics during the solar eclipse of 22 July 2009. J. Geophys. Res. 117, A11310.

Phanikumar, D.V., Kwak, Y.S., Patra, A.K., Maurya, A.K., Singh, R., Parke, S.M., 2014. Response of the mid-latitude D-region ionosphere to the total solar eclipse of 22 July 2009 studied using VLF signals in South Korean peninsula. Adv. Space Res. 54 (6), 961–968.

Prölss, G.W., 1993. Common origin of positive ionospheric storms at middle latitudes and the geomagnetic activity effect at low latitudes. J. Geophys. Res. 98, 5981–5991.

Rao, S., Chakraborty, M., Singh, A.K., 2021. A Study on TEC Reduction during the Tail Phase of the 21st June 2020 Annular Solar Eclipse S. Adv. Space Res. 67 (6), 1948–1957.

Rycroft, M.J., Reeve, C.D., 1970. VLF radio signal observed in Newfoundland during the Solar eclipse of March 7. Nature 226, 1126–1127.

Sharma, S., Dashora, N., Galav, P., Pandey, R., 2010. Total solar eclipse of July 22, 2009: Its impact on the total electron content and ionospheric electron density in the Indian zone. J. Atmos. Solar-Terr. Phys. 72, 1387–1392.

Singh, A.K., Singh, R.P., 1996. Propagation features of higher harmonic tweeks at low latitude. Earth Moon Planet 73, 277–290.

Singh, A.K., Singh, R., Veenadhari, B.V., Singh, A.K., 2012. Response of low latitude D- region ionosphere to the total solar eclipse of 22 July 2009 deduced from ELF/VLF analysis. Adv. Space Res. 50, 1352–1361.

Singh, A.K., Singh, S.B., Singh, R., Gokani, S., Singh, A.K., Siingh, D., Lichtenberger, J., 2014. Whistlers detected and analyzed by Automatic Whistler Detector (AWD) at low latitude Indian stations. J. Atmos. Sol. Terr. Phys. 121, 221–228.

Singh, S.B., Rao, S.S., Singh, A.K., 2019. Day time whistlers observed at low latitude Varanasi (L=1.078). J. Astrophys. Astron. 40, 49.

Singh, R., Veenadhari, B., Maurya, A., Cohen, M.B., Kumar, S., Selvakumaran, R., Pant, P., Singh, A.K., Inan, U.S., 2011. D-region ionosphere response to the Total Solar Eclipse of 22 July 2009 deduced from ELF-VLF tweek observations in the Indian sector. J. Geophys. Res. 116. https://doi.org/10.1029/2011JA016641.

Silwal, A., Gautam, S.P., Poudel, P., Karki, M., Adhikari, B., Chapagain, N.P., Mishra, R.K., Ghimire, B.D., Migoya-Orue, Y., 2010. Global Positioning System Observations of Ionospheric Total Electron Content Variations During the 15th January 2010 and 21st June 2020 Solar Eclipse. J. Geophys. Res. 56 (5).

Smith, L.G., 1972. Rocket observations of solar UV radiation during the eclipse of 7 March 1970. J. Atmosph. Solar –Terrest. Phys. 34 (4), 601–611.

Srivastava, G.P., Pakkir, M.P.M., Balwalli, R.R., 1982. Ozone concentration measurements near the ground at Raichur during the solar eclipse of 1980. Proc. Ind. Nat. Sci. Acad. A48 (3), 138–142.

Thomson, N.R., 1993. Experimental daytime VLF ionospheric parameters. J. Atmos. Terr. Phys. 55, 173–184.

Venkatesh, K., Rama Rao, P.V.S., Saranya, P.L., Prasad, D.S.V.V.D., Niranjan, K., 2011. Vertical electron density and topside effective scale height (H_T) variations over the Indian equatorial and low latitude stations. Ann. Geophys. 29, 1861–1872.

Venkatesham, K., Singh, R., Maurya, A.K., Dubey, A., Kumar, S., Phanikumar, D.V., 2019. The 22 July 2009 Total Solar Eclipse: Modeling D Region Ionosphere Using Narrowband VLF Observations. J. Geophys. Res. Space Phys. 124, 616–627.

Vijay Kumar, K., Maurya, A.K., Kumar, S., Singh, R., 2016. 22 July 2009 Total Solar Eclipse induced gravity waves in ionosphere as inferred from GPS observations over EIA. Adv. Space Res. 18 (9), 1755–1762.

Wait, J.R., Spies, K.P., 1964. Characteristics of the Earth ionosphere waveguide for VLF radio waves, NBS Tech. Note *U.S.* 300.

West, K.H., Goldsmith, G., Campbell, D., Zandstra, S., 1980. Effects of the 16 February 1980 solar eclipse on the composition of the low latitude ionosphere as seen by Atmosphere Explorer E. J. Geophys. Res. 113.

Yamashita, M., 1978. Propagation of tweek atmospherics. J. Atmos. Terr. Phys. 40, 155–156.

Zanis, P., Katragkou, E., Kanakidou, M., Psiloglou, B.E., Karathanasis, S., Vrekoussis, M., Gerasopoulos, E., Lysaridis, I., Markakis, K., Poupkou, A., Amiridis, V., Melas, D., Mihalopoulos, N., Zerefos, C., 2007. Effects on surface atmospheric photooxidants over Greece during the total solar eclipse event of 29 March 2006. Atmos. Chem. Phys. 7, 6061–6073.

Zerefos, C.S., Balis, D.S., Meleti, C., Bais, A.F., Tourpali, K., Vanicek, K., Cappelani, F., Kaminski, U., Tiziano, C., Stubi, R., Formenti, P., Andreae, A., 2000. Changes in environmental parameters during the solar eclipse of 11 August 1999, over Europe. Effects on surface UV 20 solar irradiance and total ozone. J. Geophys. Res. 105 (D21), 26463.

Zerefos, C.S., Gerasopoulos, E., Tsagouri, I., Psiloglou, B.E., Belehaki, A., Herekakis, T., Bais, A., Kazadzis, S., Eleftheratos, C., Kalivitis, N., Mihalopoulos, N., 2007. Evidence of gravity waves into the atmosphere during the March 2006 total solar eclipse. Atmos. Chem. Phys. 7, 4943–4951.

Zhang, S.R., Holt, J.M., Zalucha, A.M., Amory-Mazaudier, C., 2004. Midlatitude ionospheric plasma temperature climatology and empirical model based on Saint Santin incoherent scatter radar data from 1966 to 1987. J. Geophys. Res. 109, A11311.

Zhang, X.-F., Du, R.Y., Gu, S.-M., Wu, T., Wang, Y.-N., 2011. Anomalous variation of VLF signals in the total solar eclipse of 22 July 2009. Chin. Astron. Astrophys. 35, 54–61.